Supporting Information

Ultrasound *versus* Light: Exploring of photo-physicochemical and sonochemical properties of phthalocyanine-based therapeutics, theoretical study, and *in vitro* evaluations

Emre Güzel[a,b] *, Göknur Yaşa Atmaca[c], Aleksey E. Kuznetsov[d], Aysegul Turkkol[e], Mehmet Dincer Bilgin[e], Ali Erdoğmuş[b] *

[a] *Department of Engineering Fundamental Sciences, Faculty of Technology, Sakarya University of Applied Sciences, 54050, Sakarya, Turkey*

[b] *Biomedical Technologies Application and Research Center (BIYOTAM), Sakarya University of Applied Sciences, 54050, Sakarya, Turkey*

[c] *Department of Chemistry, Yıldız Technical University, 34220, İstanbul, Turkey*

[d] *Department of Chemistry, Universidad Técnica Federico Santa Maria, Av. Santa Maria 6400, Campus Vitacura, 7660251, Santiago, Chile*

[e] *Department of Biophysics, Faculty of Medicine, Aydın Adnan Menderes University, 09010, Aydın, Turkey*

* Corresponding Authors:

* Emre Güzel (eguzel@subu.edu.tr)

* Ali Erdoğmuş (aerdog@yildiz.edu.tr)

Contents

1. Materials

All reagents and solvents were of reagent grade quality obtained from commercial suppliers. The homogeneity of the products was tested in each step by TLC. The solvents were stored over molecular sieves. All solvents were dried and purified as described by Perrin and Armarego.[1]

2. Equipment

IR spectra were recorded on a Perkin Elmer Spectrum One FT-IR (ATR sampling accessory) spectrophotometer, electronic spectra on Shimadzu UV-1280 spectrophotometer. ^{1}H NMR and ^{13}C NMR spectra were recorded on Agilent VNMRS 300 MHz and the spectrum was referenced internally by using the residual solvent resonances (d = 7.26 for $CDCl_3$ in ^{1}H NMR) and chemical shifts were reported relative to Me_4Si as internal standard. Mass analyses were recorded on a Bruker MALDI-TOF (Matrix-Assisted Laser Desorption/Ionization-Time-Of-Flight mass, Rheinstetten, Germany) spectrometer using alpha-cyano-4-hydroxy-cinnamic acid (CHCA) and dithranol (DIT) as matrix materials. Elemental analyses were performed in TÜBİTAK Marmara Research Centre. Fluorescence spectra were measured using a Varian Eclipse spectrofluorometer using 1 cm path length cuvettes at room temperature. Photo-irradiations were measured using a General Electric quartz line lamp (300W). A 600 nm glass cut-off filter (Schott) and a water filter were used to filter off ultraviolet and infrared radiations respectively. An interference filter (Intor, 700 nm with a bandwidth of 40 nm) was additionally placed in the light path before the sample. Light intensities were measured with a POWER MAX5100 (Mol electron detector incorporated) power meter. Bandelin Ultrasonic RK 100 H was used for ultrasound irradiation.

3. Characterization

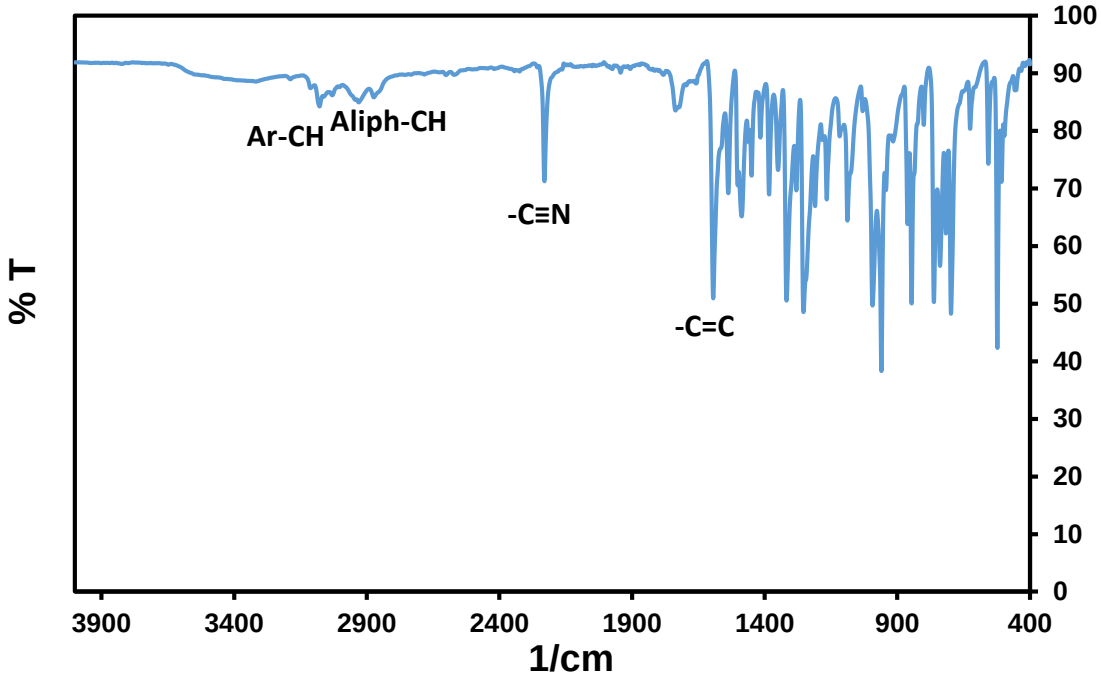

Figure S1. FT-IR spectrum of phthalonitrile compound **1**.

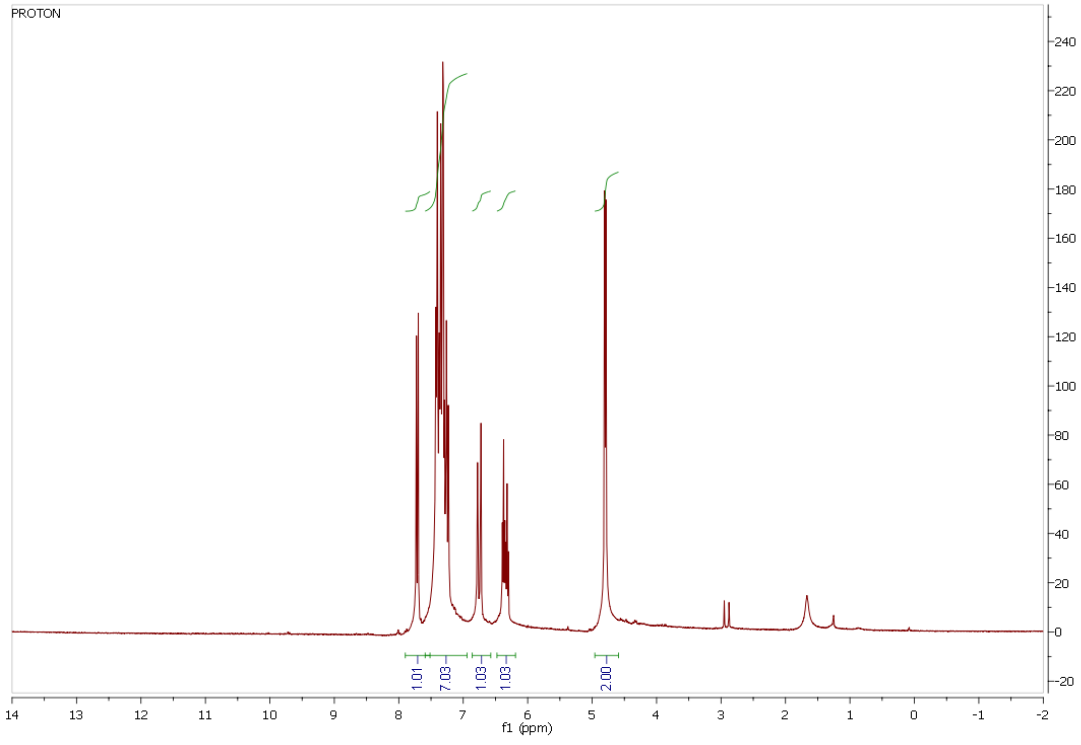

Figure S2. ^{1}H NMR spectrum of phthalonitrile compound **1** in $CDCl_3$.

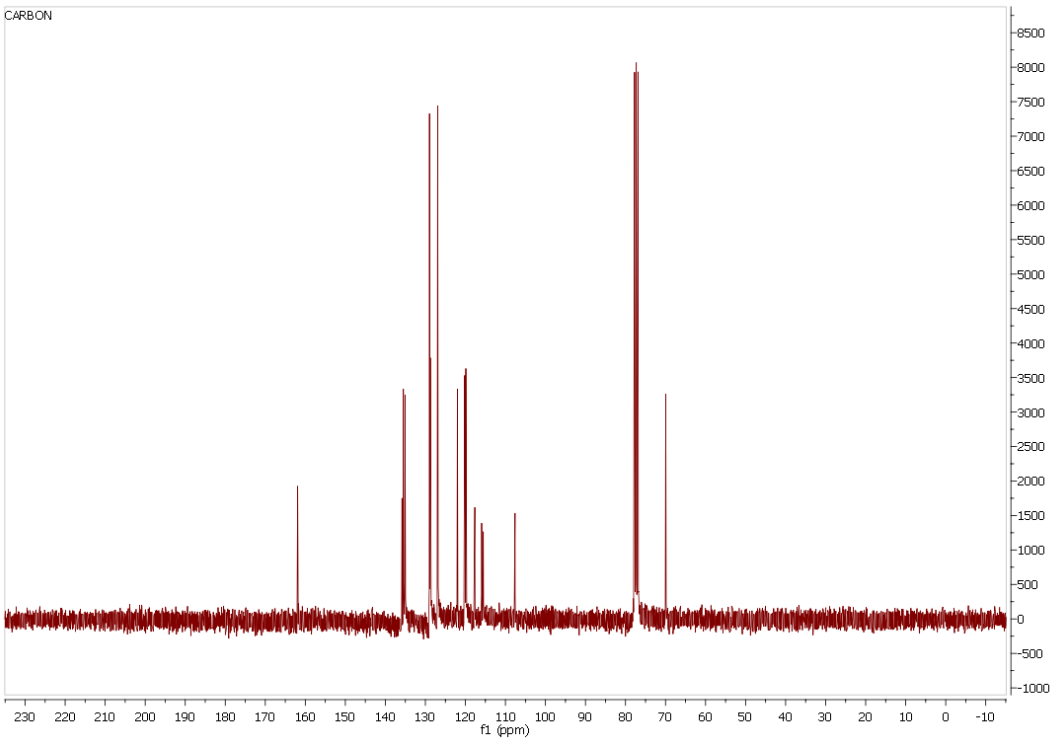

Figure S3. ^{13}C NMR spectrum of phthalonitrile compound **1** in $CDCl_3$.

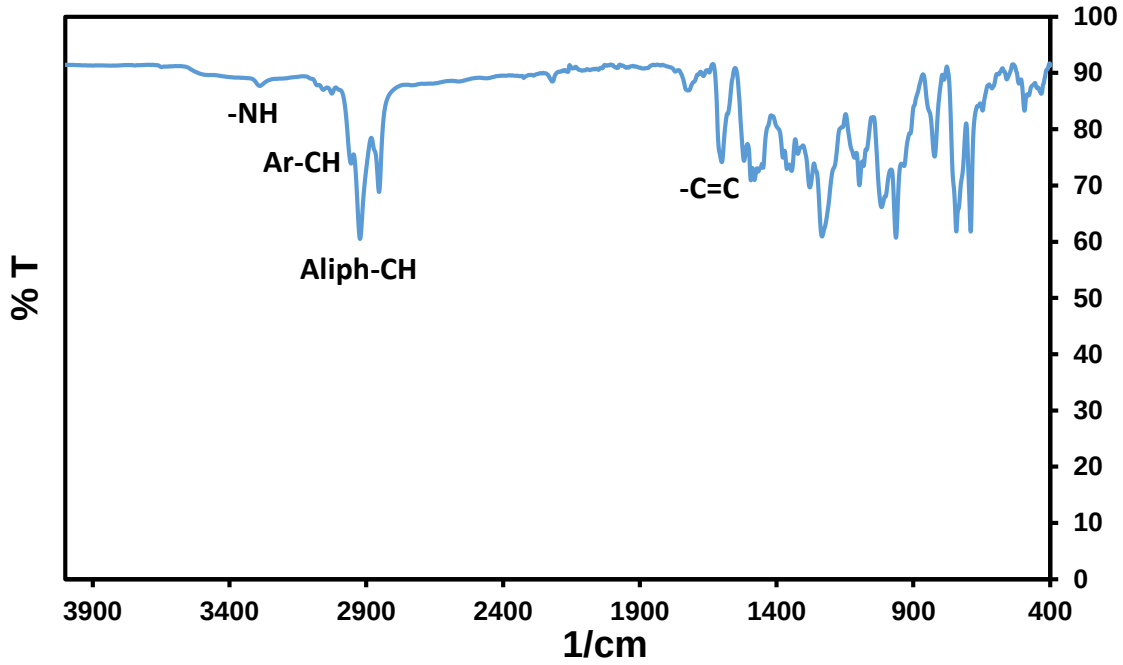

Figure S4. FT-IR spectrum of metal-free phthalocyanine (**2**).

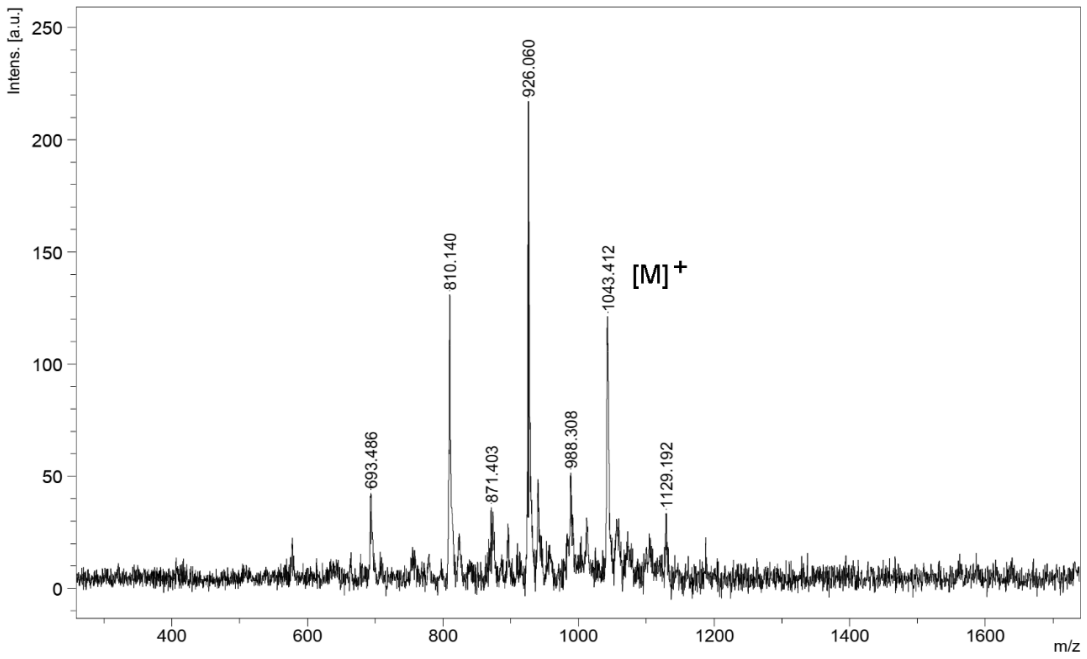

Figure S5. The MALDI-TOF mass spectrum of metal-free phthalocyanine (**2**).

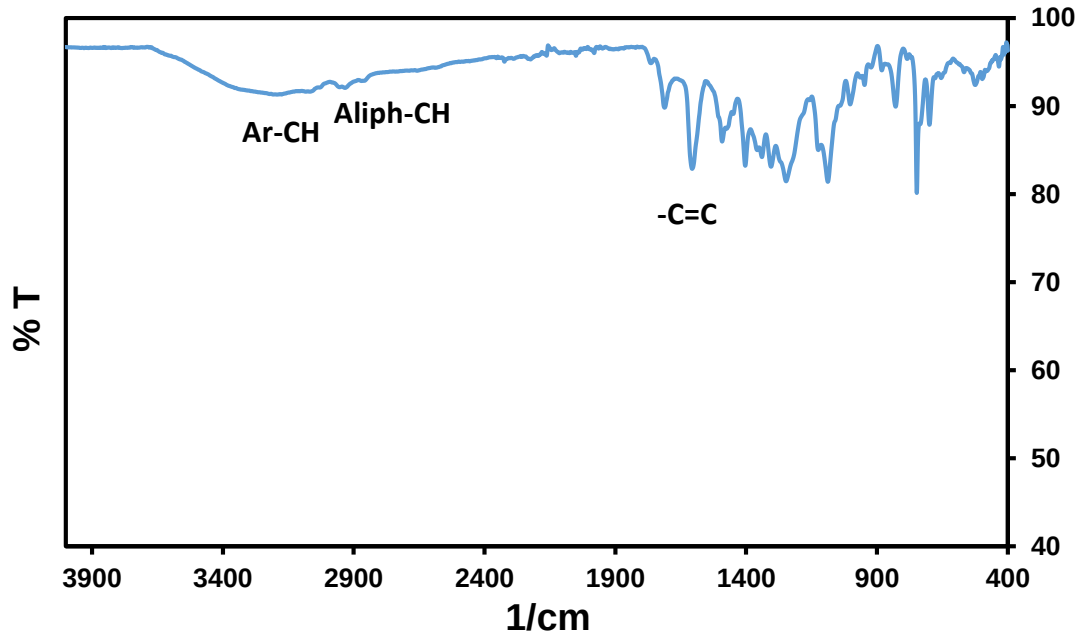

Figure S6. FT-IR spectrum of gallium phthalocyanine (**3**).

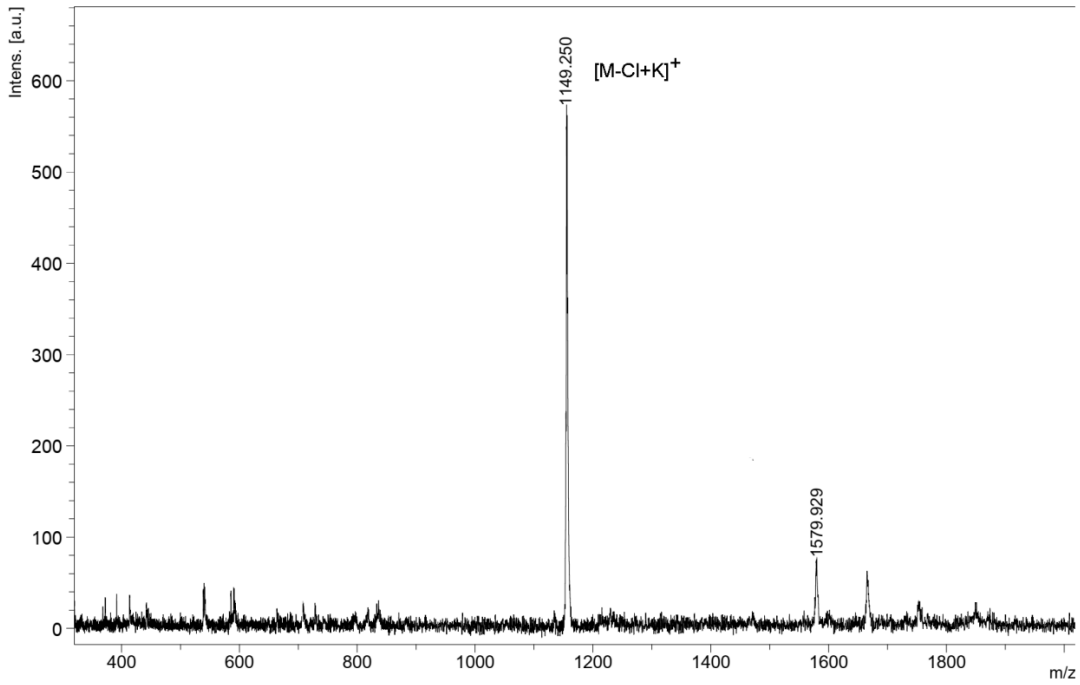

Figure S7. The MALDI-TOF mass spectrum of gallium phthalocyanine (**3**).

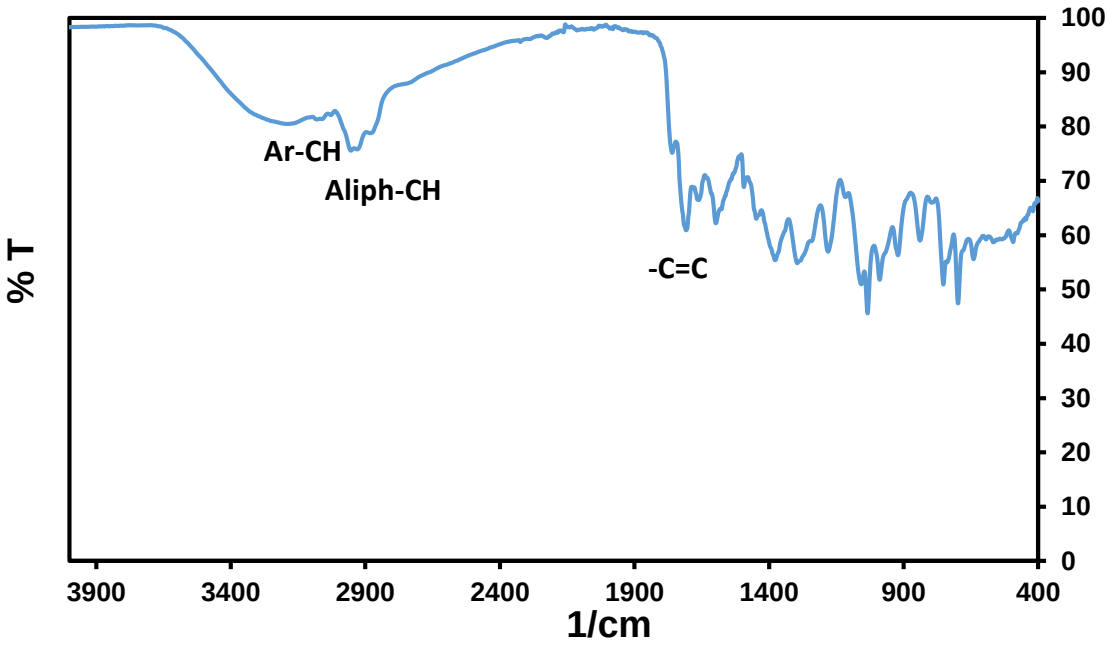

Figure S8. FT-IR spectrum of indium phthalocyanine (**4**).

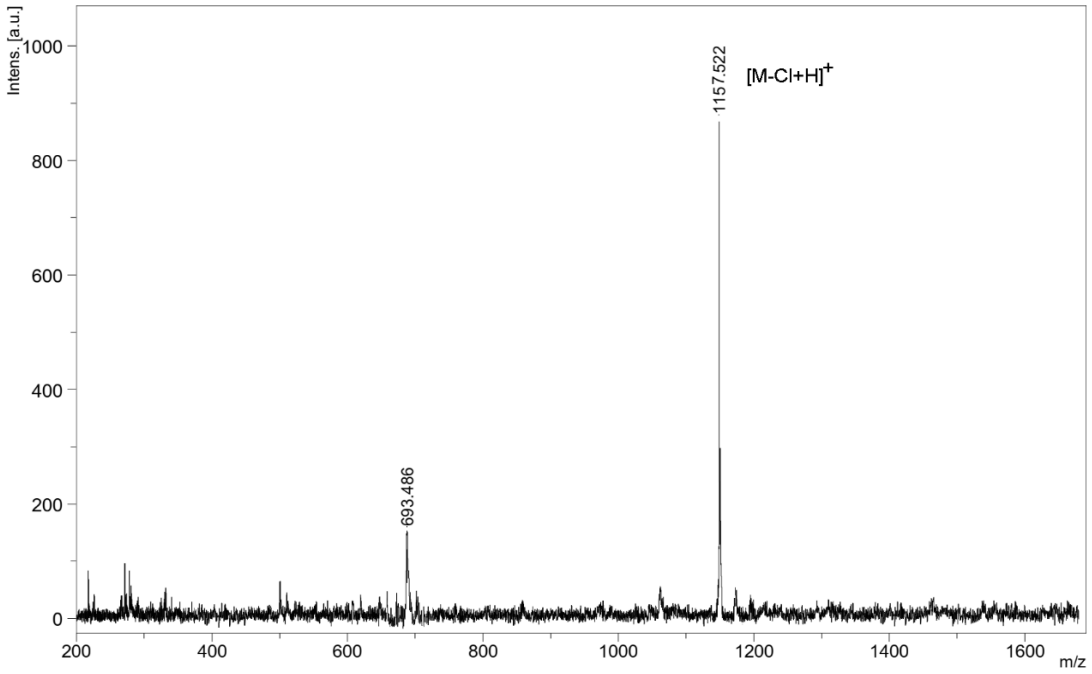

Figure S9. The MALDI-TOF mass spectrum of indium phthalocyanine (**4**).

4. Photophysical and photochemical parameters

Fluorescence excitation and emission spectra were recorded on a Shimadzu spectrofluorometer using a 1 cm path length cuvette at room temperature. Fluorescence quantum yields (Φ_F) are determined in DMSO by the comparative method using equation **1**.[2,3]

$$\Phi_F = \Phi_{F_{Std}} \frac{F * A_{Std} * \eta^2}{F_{Std} * A * \eta^2_{Std}} \quad (\mathbf{1})$$

where F and F_{Std} are the areas under the fluorescence emission curves of the samples (**4** and **5**) and the standard, respectively. A and A_{Std} are the respective absorbances of the samples and standard at the excitation wavelengths, respectively. n^2 and n^2_{Std} are the refractive indices of solvents used for the sample and standard, respectively. Reference (unsubstituted) ZnPc (Φ_F = 0.20)[4] was employed as the standard in DMSO. The absorbance of the solutions at the excitation wavelength ranged between 0.04 and 0.05. Both the samples and standards were excited at the same wavelength.

Singlet oxygen quantum yield (Φ_Δ) determinations were carried out by using the experimental set-up described in the literature.[5–7] Typically, a 3 mL portion of the respective unsubstituted zinc (II) phthalocyanine (ZnPc) and the studied phthalocyanine solutions (C= 1x10^{-5} M) containing the singlet oxygen quencher was irradiated in the Q band region with the photo-irradiation set-up described in references.[6–9] Singlet oxygen quantum yields (Φ_Δ) were determined in THF using the relative method with unsubstituted zinc (II) phthalocyanine (ZnPc) as a reference. DPBF was used as the chemical quencher for singlet oxygen in DMSO. Equation **2** was employed for the calculations:

$$\Phi_\Delta = \Phi_\Delta^{\mathrm{Std}} \frac{\mathrm{R} * \mathrm{I}_{\mathrm{abs}}^{\mathrm{Std}}}{\mathrm{R}^{\mathrm{Std}} * \mathrm{I}_{\mathrm{abs}}} \quad (\mathbf{2})$$

where Φ_Δ^{std} is the singlet oxygen quantum yield for the standard unsubstituted zinc (II) phthalocyanine. R and R_{Std} are the DPBF photobleaching rates in the presence of studied phthalocyanine compounds and standard, respectively. $\mathrm{I}_{\mathrm{abs}}$ and $\mathrm{I}_{\mathrm{abs}}^{\mathrm{Std}}$ are the rates of light absorption by the studied phthalocyanine compounds and standard, respectively. To avoid chain reactions induced by DPBF in the presence of singlet oxygen, the concentration of quencher (DPBF) was lowered to ~5x10^{-6} M. Solutions of sensitizers (C= 1x10^{-6} M) containing DPBF were prepared in the dark and irradiated in the Q band region using the photoirradiation setup. DPBF degradation at 417 nm was monitored. The light intensity 7.05 x 10^{15} photons s^{-1} cm^{-2} was used for Φ_Δ determinations. The absorption band of DPBF is reduced by light irradiation (Figure 3). For sono-photochemical studies, the sample (the compound+DPBF) was monitored after each 10 s irradiation (5 s by light intensity of 7.05 x 10^{15} photons s^{-1} cm^{-2} and 5 s by ultrasound at a frequency of 35 kHz).

Photodegradation quantum yields were determined by the comparative method using equation **3**.

$$\Phi_{\mathrm{d}} = \frac{(\mathrm{C}_0 - \mathrm{C}_{\mathrm{t}}) * \mathrm{V} * \mathrm{N}_{\mathrm{A}}}{\mathrm{I}_{\mathrm{abs}} * \mathrm{S} * \mathrm{t}} \quad (\mathbf{3})$$

where C_0 and C_t are the sample concentrations before and after irradiation respectively, V is the reaction volume, N_A is the Avogadro's constant, S is the

irradiated cell area, t is the irradiation time, I_{abs} is the overlap integral of the radiation source light intensity and the absorption of the samples. A light intensity of 7.05 x 10^{15} photons s^{-1} cm^{-2} and/or ultrasound at a frequency of 35 kHz was employed to determine photodegradation was employed for Φ_{Δ} determinations.[10]

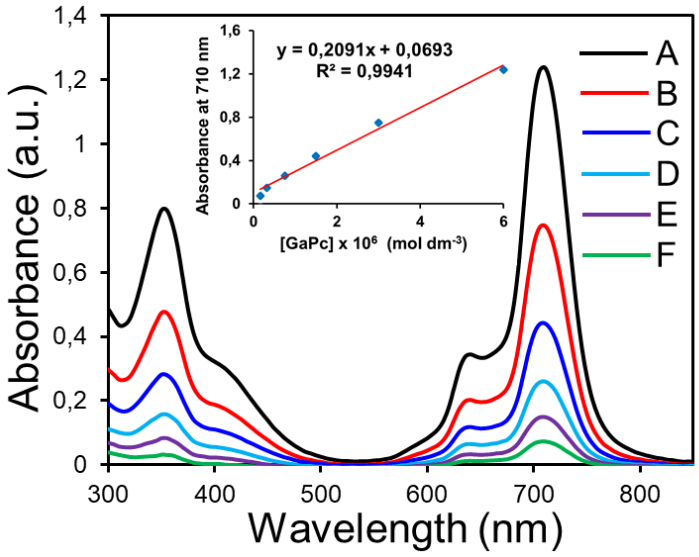

Figure S10. Absorption spectra of GaPc (**3**) in THF at different concentrations: 6 $x10^{-6}$ (A), 3 $x10^{-6}$ (B), 1.5 $x10^{-6}$ (C), 7.5 $x10^{-7}$ (D), 3.25 $x10^{-7}$ (E) and 1.63 $x10^{-7}$ $mol.dm^{-3}$ (F). Figure S10 shows the UV-vis spectra of GaPc (**3**) in THF at various concentrations. The lack of aggregation was proved by absorption studies performed at a range of concentrations. For the verification of the Lambert-Beer law, an analysis of linear regression between the intensity of the Q-band and the concentration of the GaPc (**3**) showed R^2 value. The Q-band strictly followed the Lambert-Beer law, suggesting that it is essentially free from aggregation in THF.

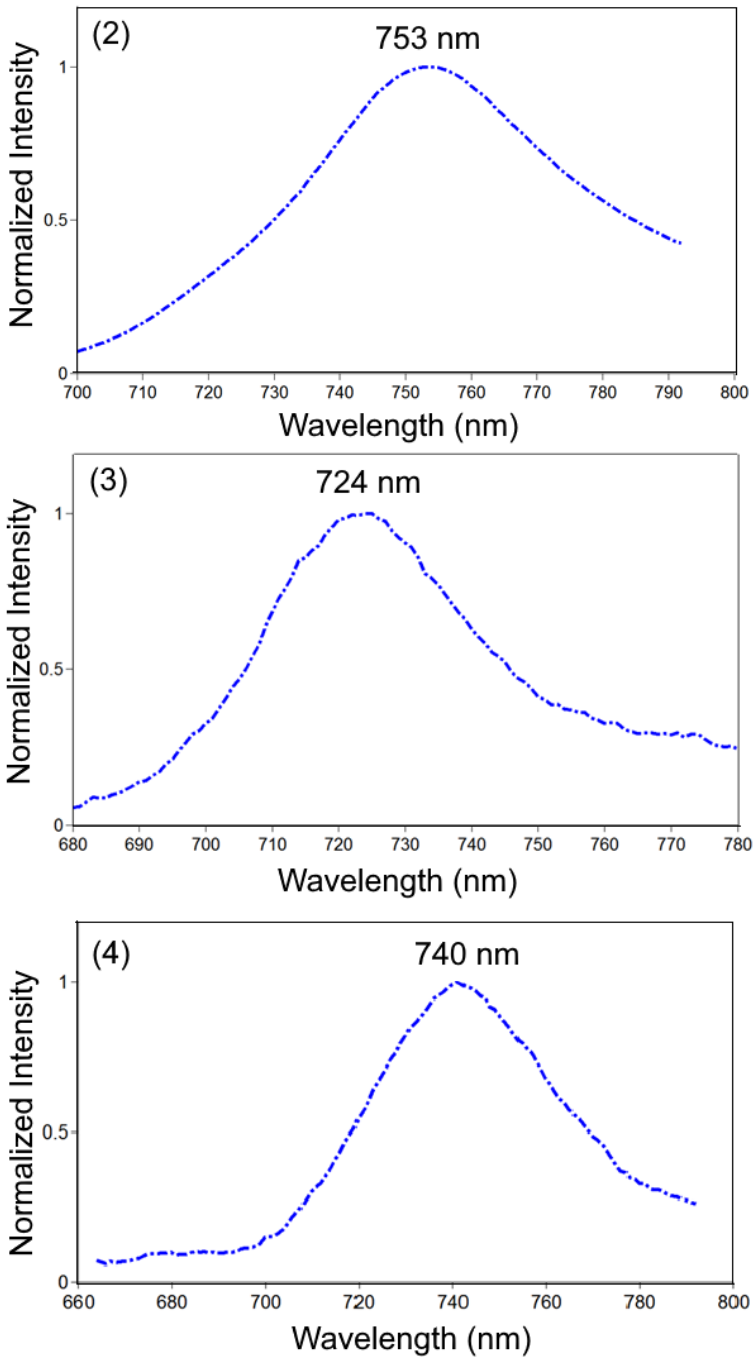

Figure S11. Emission spectra of the phthalocyanines (**2**-**4**) in DMSO.

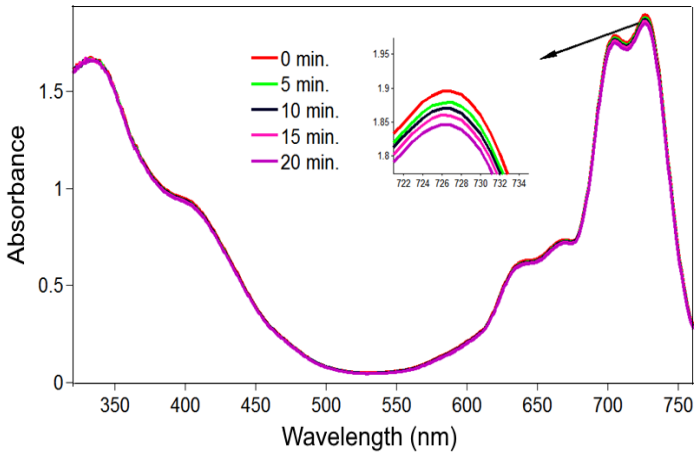

Figure S12. A typical spectrum for the determination of photodegradation of metal-free phthalocyanine (**2**) in DMSO.

5. Theoretical calculations

Table S1. Computational results, gas phase//THF.

Compound	E_0, A.U.	E_0+ZPE, A.U.	ΔE, kcal/ mol	E(HOMO/LUMO), A.U.	ΔE, eV/ TDDFT, eV
B3LYP/6-31G*					
2, ^{1}A	-3360.237506// -3360.261201	-3359.212222// -3359.236064	0.0// 0.0	-0.16758/ -0.09220// -0.17859/ -0.10418	2.05/ 2.02/1.88[a], 1.80[b]
2, ^{3}A	-3360.202715// -3360.226600	-3359.180169// -3359.204304	21.83// 21.71	-0.13272/ -0.08334 -0.20823/ -0.12756// -0.14602/ -0.09608 -0.21972/ -0.14020	
3, ^{1}A	-5742.364802// -5742.390846	-5741.358695 // -5741.385189	0.0// 0.0	-0.17164/ -0.09698// -0.18328/ -0.10985	2.03/ // 2.00/1.83[a], 1.75[b]
3, ^{3}A	-5742.328484// -5742.356626	-5741.324834// -5741.352933	22.79// 21.47	-0.13676/ -0.09255 -0.21805/ -0.13389// -0.15050/ -0.10598 -0.22692/ -0.14656	
B3LYP/Gen					
4, ^{1}A,	-9536.632095// -9536.658298	-9535.627731// -9535.654090	0.0// 0.0	-0.17353/ -0.09874// -0.18340/ -0.10969	2.04/ // 2.01/1.83,[a]

					1.76[b]
4, ^{3}A,	-9536.596048 5i// -9536.623459	-9535.593975// -9535.621520	22.62// 21.86	-0.13853/ -0.09332 -0.21812/ -0.13540// -0.15044/ -0.10546 -0.22608/ -0.14678	
4, ^{1}A, B3LYP/ [In:SDD; C,H,O,N,Cl: 6-31G*]	-3821.248692	-3820.244581		-0.18382/ -0.11037	
B3LYP/6-311G(d,p)					
2, ^{1}A	-3361.033976// -3361.059169	-3360.016073// -3360.041319	0.0// 0.0	-0.17598/ -0.10100// -0.18668/ -0.11260	2.04/ // 2.02/1.86[a],
2, ^{3}A	-3360.998970// -3361.025134	-3359.983645// -3360.009778	21.97// 21.36	-0.14187/ -0.09192 -0.21722/ -0.13626// -0.15460/ -0.10402 -0.22823/ -0.14834	
3, ^{1}A	-5745.083911// -5745.113126	-5744.085517// -5744.114750	0.0// 0.0	-0.18047/ -0.10602// -0.19106/ -0.11778	2.03/ // 1.99/1.82[a],
3, ^{3}A	-5745.047843// -5745.078198	-5744.051852// -5744.082075	22.63// 21.92	-0.14599/ -0.10140 -0.22685/ -0.14284// -0.15881/ -0.11392 -0.23552/ -0.15467	
B3LYP/Gen1					
4, ^{1}A	-9537.524414// -9537.553624	-9536.527383// -9536.556778	0.0// 0.0	-0.18239/ -0.10775// -0.19129/ -0.11765	2.03/ // 2.00/
4, ^{3}A	-9537.488638// -9537.518602	-9536.493771// -9536.523927	22.45// 21.98	-0.14788/ -0.10207 -0.22730/ -0.14433// -0.15903/ -0.11297 -0.23480/ -0.15465	

[a]TD-B3LYP
[b]TD-wB97XD

Table S2. TDDFT results for the compounds **2-4**, implicit THF, TD-B3LYP//TD-ωB97XD.

Excited state	E, eV	λ, nm	Oscillator strength, f	Transition(s)
2				
1	1.8811// 1.8008	659.11// 688.50	0.7216// 0.7517	HOMO → LUMO HOMO → LUMO+1// HOMO-9 → LUMO HOMO → LUMO HOMO → LUMO+1
2	1.9121// 1.8307	648.43// 677.24	0.7187// 0.8129	HOMO-9 → LUMO HOMO → LUMO HOMO → LUMO+1// HOMO → LUMO HOMO → LUMO+1
3	2.7069// 3.3821	458.0// 366.59	0.0000// 0.2601	HOMO-4 → LUMO HOMO-1 → LUMO HOMO-1 → LUMO+1// HOMO-9 → LUMO HOMO-6 → LUMO HOMO-3 → LUMO HOMO-2 → LUMO HOMO-2 → LUMO+1 HOMO-1 → LUMO+2
3				
1	1.8258// 1.7471	679.05// 709.64	0.6460// 0.7123	HOMO → LUMO HOMO → LUMO+1// HOMO-13 → LUMO+1 HOMO → LUMO
2	1.8263// 1.7475	678.86// 709.51	0.6459// 0.7129	HOMO → LUMO HOMO → LUMO+1// HOMO-13 → LUMO+1 HOMO → LUMO+1
3	2.8047// 3.5592	442.06// 348.35	0.1314// 0.0003	HOMO-5 → LUMO HOMO-5 → LUMO+1

				HOMO-3 → LUMO HOMO-2 → LUMO HOMO-1 → LUMO HOMO-1 → LUMO+1// HOMO-7 → LUMO HOMO-7 → LUMO+1 HOMO-6 → LUMO HOMO-6 → LUMO+1 HOMO → LUMO+2 HOMO → LUMO+3
4				
1	1.8345// 1.7553	675.83// 706.35	0.6611// 0.7301	HOMO → LUMO HOMO → LUMO+1// HOMO-13 → LUMO+1 HOMO → LUMO HOMO → LUMO+1
2	1.8349// 1.7555	675.69// 706.25	0.6610// 0.7297	HOMO → LUMO HOMO → LUMO+1// HOMO-13 → LUMO+1 HOMO → LUMO HOMO → LUMO+1
3	2.7725// 3.5280	447.20// 351.43	0.1280// 0.0032	HOMO-5 → LUMO HOMO-3 → LUMO HOMO-1 → LUMO// HOMO-8 → LUMO+2 HOMO-7 → LUMO HOMO-7 → LUMO+1 HOMO-6 → LUMO HOMO-6 → LUMO+1 HOMO-5 → LUMO HOMO-2 → LUMO+1 HOMO → LUMO+2

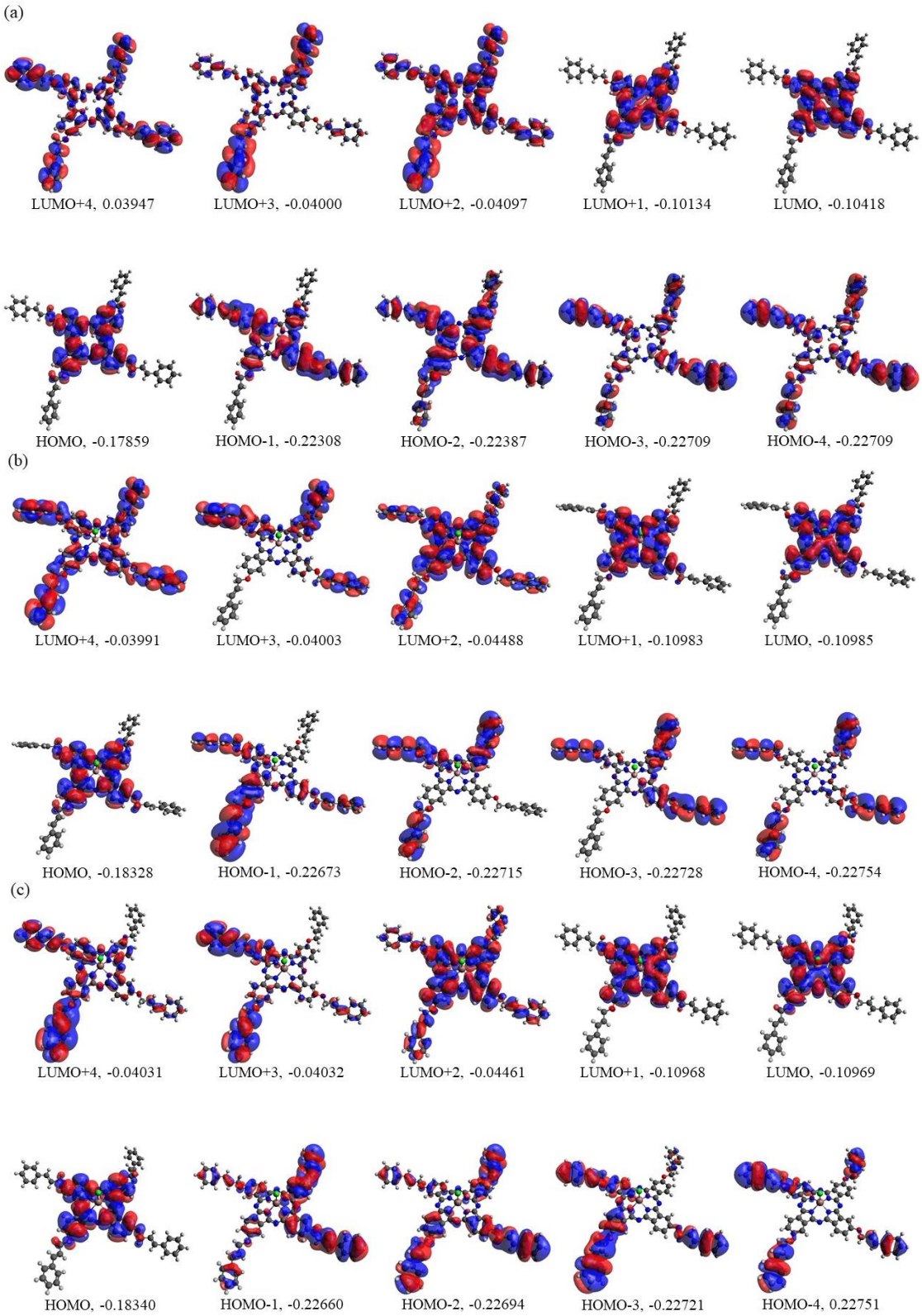

Figure S13. Molecular orbitals from HOMO-4 to LUMO+4 for the compounds 2 (a), 3 (b), and 4 (c), calculated in the implicit THF with the B3LYP/6-31G* (B3LYP/Gen) approach.

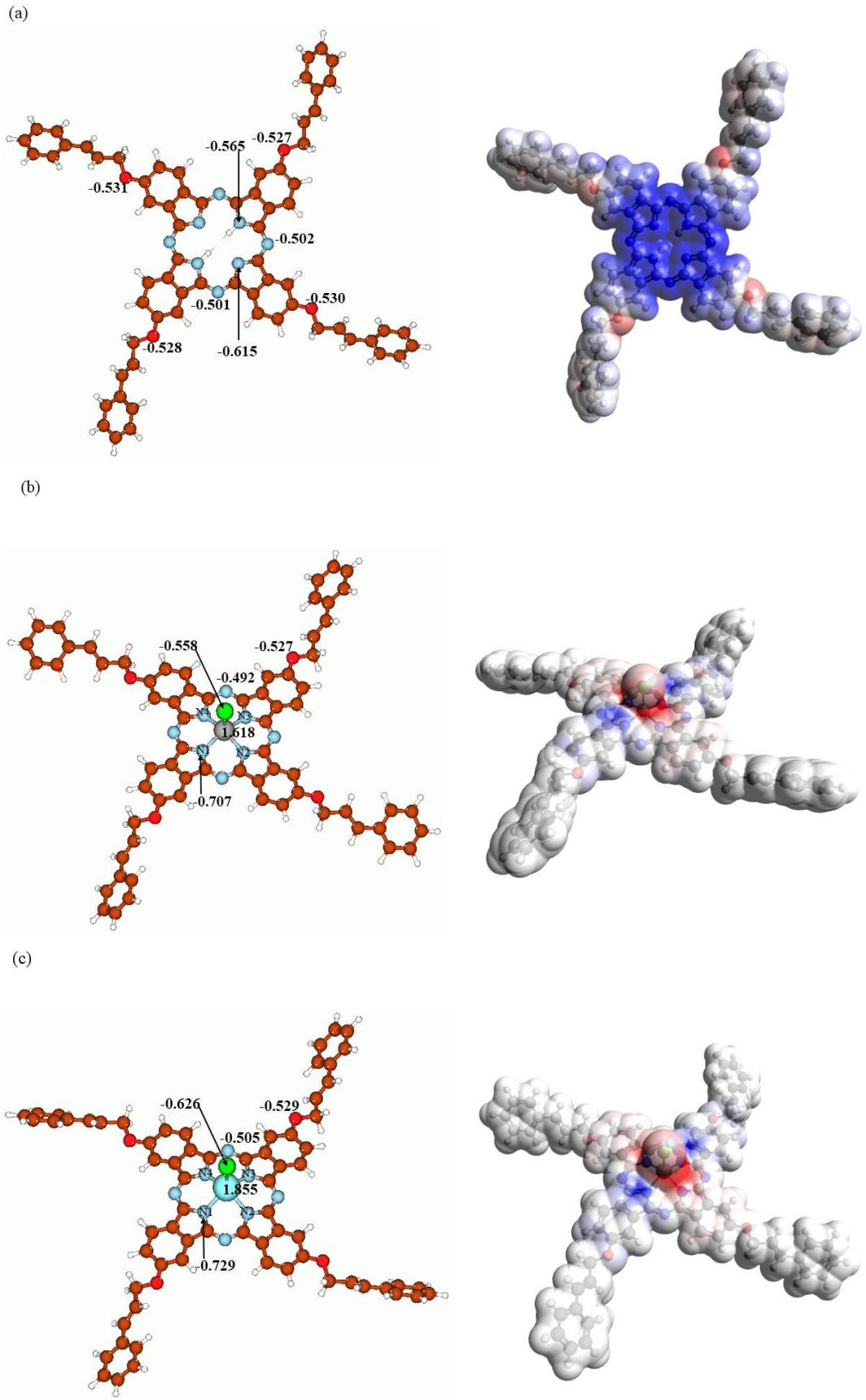

Figure S14. Selected NBO charges (left) and plots of molecular electrostatic potential (right) for the compounds **2** (a), **3** (b), and **4** (c), computed at the B3LYP/6-31G* (B3LYP/Gen) level in the implicit THF.

6. *In vitro* studies

Sonophotodynamic therapy (SPDT) uses the light of a particular wavelength and sound of a particular frequency to activate sono-photosensitizers to generate reactive oxygen species in the presence of molecular oxygen that lead to cancer cell death. However, light or ultrasound alone did not produce a therapeutic effect.[11] Various doses of ultrasound or light applied alone did not affect the cell viability of MKN-28 gastric cancer cells (Figure S15).

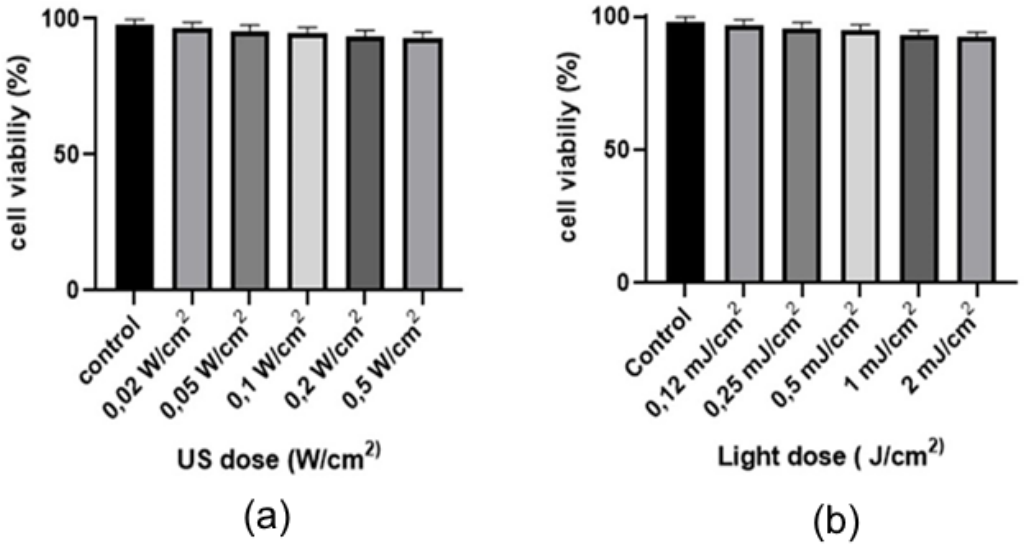

Figure S15. The cell viabilities of MKN-28 gastric cancer cells in (a) ultrasound alone and (b) light alone groups.

The Muse Oxidative Stress Kit® was used to show the amount of intracellular ROS. The assay provides the relative percentage of cells that are ROS negative and positive in both adherent cells and cells in suspension on the Guava Muse Cell Analyzer. A significant increase in intracellular ROS was found in the MKN-28 gastric cancer cells after they were treated with PDT, SDT, and SPDT when compared to the control (Figure S16).

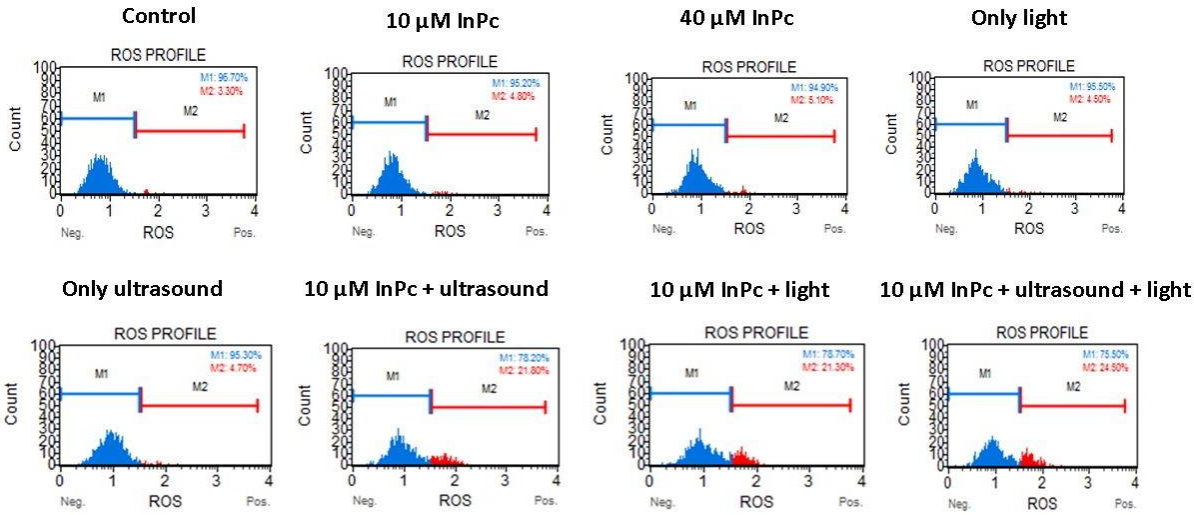

Figure S16. The quantitative measurement of cells undergoing oxidative stress was evaluated by cytometry, using the Muse Oxidative Stress Kit. The graph showed the positive ROS percentage in the different groups.

The effect of various concentrations of phthalocyanines (2,5,10,20,40 µM) and their treatment groups (SDT, PDT, and SPDT) on cell viabilities of MKN-28 gastric cancer cell lines was shown in Table S3. The 40 µM of GaPc (**3**) and InPc (**4**) reduced cell viability of MKN-28 gastric cancer cells to74.38±1 % and 54.63±2%, respectively while the same concentration of H_2Pc (**2**) decreased cell viability of gastric cancer cells to 95.22±1%. The results show that metal ions affect the cell viabilities of phthalocyanines. Furthermore, treatments groups decreased the cell viabilities of gastric cancer cells. After the ultrasound or /and light treatments, both H_2Pc (**2**) and GaPc (**3**) showed the cytotoxic effect to MKN-28 cancer cells with InPc (**3**) highly cytotoxic at all concentrations.

Table S3. Cell viability results of various concentration of H_2Pc (**2**), GaPc (**3**) and InPc (**4**) alone with only drug groups and phthalocyanines mediated treatment groups (Mean ± standard error of the mean)

Concent.	Only Drug			SDT			PDT			SPDT		
μM	H_2Pc	GaPc	InPc	H_2Pc	GaPc	InPc	H_2Pc	GaPc	InPc	H_2Pc	GaPc	InPc
2	97.56 ±3	92.33 ±3	92.25 ±3	97.0 ±3	85,25 ±3	90,11 ±2	87,56 ±4	87,75 ±4	79.0 ±2	86,22 ±4	84,75 ±2	74.0 ±1
5	97.0 ±3	87.0 ±3	82.56 ±1	96.88 ±3	80,5 ±4	83,22 ±1	85,78 ±4	83,25 ±3	68.75 ±3	81.0 ±3	81,5 ±3	65.5 ±2
10	96.89 ±2	85.75 ±3	80.0 ±1	96,11 ±3	76,38 ±2	78,11 ±2	84,89 ±4	79,25 ±3	65.0 ±1	80,89 ±2	73,75 ±2	58,67 ±3
20	96.11 ±1	76.0 ±3	76.63 ±3	94,33 ±2	73,13 ±2	74.85 ±3	82,56 ±2	72.57 ±3	51.28 ±2	76,11 ±2	69,88 ±3	41.0 ±2
40	95.22 ±1	74.38 ±1	54.63 ±2	93.38 ±3	72,88 ±1	49,44 ±1	80,89 ±2	71.5 ±2	47.0 ±1	74,33 ±1	67,63 ±2	37.4 ±2

Photodynamic therapy (PDT), sonodynamic therapy (SDT) and sonophotodynamic therapy (SPDT) demonstrate their effects by generating ROS that lead to cell death. Therefore, ROS level is an important parameter to evaluate the effects of the treatments. InPc (**4**) mediated photo-, sono-, sonophoto-dynamic therapies significantly increase the ROS production on MKN28 gastric cancer cells (Figure S17). When the results are examined, it is seen that ultrasound and light alone do not have a significant difference compared to the control. After adding the InPc (**4**), it is seen that the light and ultrasound applications have a significant difference compared to the control.

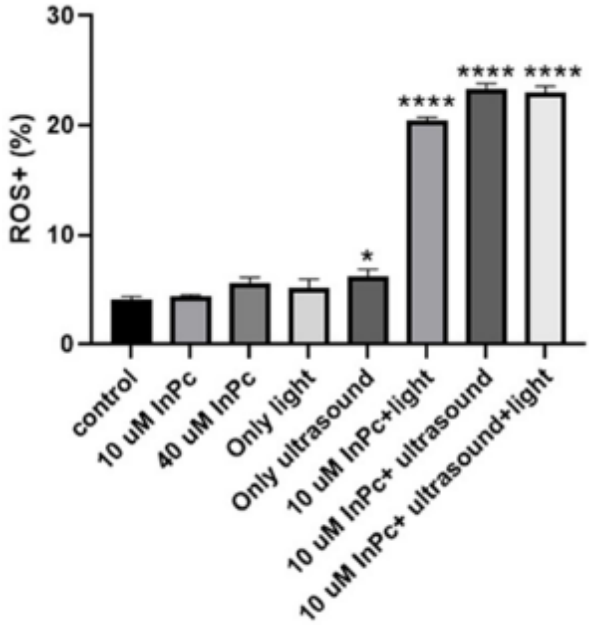

Figure S17. The percentage of ROS in the application groups. P values equal or less than 0.05 were considered as statistically significant versus untreated control (*p <; 0.05, **p<; 0.01, ***p <; 0.001, ****p<; 0.0001).

References

(1) Perrin DD, Armarego WLF. *Purification of Laboratory Chemicals (2nd Edn)*, Pergamon P.; Oxford, 1989.

(2) Güzel, E.; Arslan, B. S.; Atmaca, G. Y.; Nebioğlu, M.; Erdoğmuş, A. High Photosensitized Singlet Oxygen Generating Zinc and Chloroindium Phthalocyanines Bearing (4-Isopropylbenzyl)Oxy Groups as Potential Agents for Photophysicochemical Applications. *ChemistrySelect* **2019**, *4* (2), 515–520. https://doi.org/10.1002/slct.201803255.

(3) Maree, M. D.; Nyokong, T.; Suhling, K.; Phillips, D. Effects of Axial Ligands on the Photophysical Properties of Silicon Octaphenoxyphthalocyanine. *J. Porphyr. Phthalocyanines* **2002**, *06* (06), 373–376. https://doi.org/10.1142/S1088424602000452.

(4) Ogunsipe, A.; Chen, J.; Nyokong, T. Photophysical and Photochemical Studies of Zinc (II) Phthalocyanine Derivatives—Effects of Substituents and Solvents. *New J. Chem.* **2004**, *28* (7), 822–827. https://doi.org/10.1039/B315319C.

(5) Ogunsipe, A.; Nyokong, T. Photophysical and Photochemical Studies of Sulphonated Non-Transition Metal Phthalocyanines in Aqueous and Non-Aqueous Media. *J. Photochem. Photobiol. A* **2005**.

(6) Brannon, J. H.; Magde, D. Picosecond Laser Photophysics. Group 3A Phthalocyanines. *J. Am. Chem. Soc.* **1980**, *102* (1), 62–65. https://doi.org/10.1021/ja00521a011.

(7) Seotsanyana-Mokhosi, I.; Kuznetsova, N.; Nyokong, T. Photochemical Studies

of Tetra-2,3-Pyridinoporphyrazines. *J. Photochem. Photobiol. A Chem.* **2001**, *140* (3), 215–222. https://doi.org/10.1016/S1010-6030(01)00427-0.

(8) Güzel, E. Dual-Purpose Zinc and Silicon Complexes of 1,2,3-Triazole Group Substituted Phthalocyanine Photosensitizers: Synthesis and Evaluation of Photophysical, Singlet Oxygen Generation, Electrochemical and Photovoltaic Properties. *RSC Adv.* **2019**, *9* (19), 10854–10864. https://doi.org/10.1039/C8RA10665G.

(9) Ogunsipe, A.; Nyokong, T. Photophysical and Photochemical Studies of Sulphonated Non-Transition Metal Phthalocyanines in Aqueous and Non-Aqueous Media. **2005**, *173* (2), 211–220. https://doi.org/10.1016/J.JPHOTOCHEM.2005.03.001.

(10) Kırbaç, E.; Atmaca, G. Y.; Erdoğmuş, A. Novel Highly Soluble Fluoro, Chloro, Bromo-Phenoxy-Phenoxy Substituted Zinc Phthalocyanines; Synthesis, Characterization and Photophysicochemical Properties. *J. Organomet. Chem.* **2014**, *752*, 115–122. https://doi.org/10.1016/J.JORGANCHEM.2013.12.005.

(11) Aksel, M.; Kesmez, Ö.; Yavaş, A.; Bilgin, M. D. Titaniumdioxide Mediated Sonophotodynamic Therapy against Prostate Cancer. *J. Photochem. Photobiol. B Biol.* **2021**, *225*, 112333. https://doi.org/10.1016/J.JPHOTOBIOL.2021.112333.